

**Study on the Synergistic Enhancement of Photocatalytic
Degradation of Carbendazim by Co doped BiOBr induced Spin
Polarization and OVs**

*Hongyu Wang^{a,b}, Yuan Wei^a, Chao Liu^a, Jiaxian Li^a, Xin Li^a, Yang Yang^a, Tiantian Wang^a,
Yulan Zhang^a, Yanyan Jiang, Gaofeng Shi^{a,*}, Guoying Wang^{a,b,*}*

^a College of Petrochemical Technology, Lanzhou University of Technology, Lanzhou 730050, China

^b School of Petrochemical Engineering, Lanzhou Petrochemical University of Vocational Technology, 730060
Lanzhou, Gansu, China

^c HeXi University, Zhangye 734000, PR China

**Corresponding Authors.*

Dr. Gaofeng Shi

E-mail: gaofengshi_lzh@163.com

Dr. Guoying Wang

E-mail: wangguoying@lut.edu.cn

Text S1. Reagents.

Text S2. Characterization.

Text S3. Theoretical calculations.

Table S1. Crystallite size of BiOBr and 5% Co-BiOBr samples by using Debye-Scherrer.

Table S2. Comparison of the photocatalytic performance of related catalysts in the degradation of CBZ.

Table S3. Fluorescence lifetime parameters of the samples.

Figure S1. XPS survey spectra of BiOBr and 5% Co-BiOBr.

Text S1. Reagents

Carbendazim ($\geq 98\%$), Ciprofloxacin ($\geq 98\%$), Levofloxacin ($\geq 98\%$), Tetracycline ($\geq 98\%$), Methyl Orange ($\geq 98\%$), $\text{Bi}(\text{NO}_3)_3 \cdot 5\text{H}_2\text{O}$, KBr, AgNO_3 , KBrO_3 , ethylene glycol (EG), L-Histidine ($\text{C}_6\text{H}_9\text{N}_3\text{O}_2$), ammonium oxalate [$(\text{NH}_4)_2\text{C}_2\text{O}_4$], isopropyl alcohol ($\text{C}_3\text{H}_8\text{O}$), 4-Hydroxy-TEMPO ($\text{C}_9\text{H}_{18}\text{NO}_2^*$), NaCl, Na_2SO_4 , NaHCO_3 , Na_2HPO_3 and Na_2CO_3 were supplied by Macklin Biochemical Technology Co., Ltd. The deionized water was purified by the laboratory Millipore-Q System.

Text S2. Characterization

The crystalline structures were analyzed by X-ray diffraction (XRD, UltimaIV) with the Cu K α radiations. The structure and chemical bond of the catalysts were analyzed by Fourier transform infrared spectroscopy (FT-IR, Nicolet NEXUS 670). The micromorphology, lattice information, and elemental distribution of the catalysts were observed by scanning electron microscopy (SEM, Zeiss Sigma 300) and transmission electron microscopy (TEM, FEI Tecnai G2 F20). The valence state of each element in the catalysts was analyzed by X-ray photoelectron spectroscopy (XPS, Thermo Scientific K-Alpha, China). The UV-Vis diffuse reflectance spectroscopy (UV-Vis DRS, Shimadzu UV-3600i Plus) was used to measure the light absorption performance. The emission spectra photoluminescence spectra (PL, PerkinElmer-LS55) at excitation wavelength of 280 nm were measured to investigate the separation ability of photocarriers. Measurement of total organic carbon (TOC, Shimadzu TOC-L CPN CN200) was quantified with a TOC analyzer. The impedance (EIS) was tested on an electrochemical workstation (Shanghai Chenhua CHI660E). Time-resolved photoluminescence decay spectra were measured using a steady-state/transient fluorescence spectrometer (TRPL, Edinburgh FLS1000). Electron spin resonance (ESR) spectra were collected using a Bruker A300 instrument.

Text S3. Theoretical calculations

The density functional theory (DFT) calculations were carried out using the Cambridge Serial Total Energy Package (CASTEP) module. The geometry optimization and electronic structures of BiOBr, BiOBr-Ov and Co-BiOBr were calculated by the Generalized Gradient Approximation

(GGA) with Perdew-Burke-Ernzerhof (PBE) functional, with the considerations of spin-orbit polarization. For all calculations, the electronic states were expanded using a plane-wave basis set with a kinetic energy cut-off of 489.80 eV. The K-grid points was set to $1 \times 1 \times 1$ and the electronic energy, the maximum displacement, the precision of interatomic interaction force, the precision of crystal internal stress were 2.0×10^{-5} eV, 0.002 Å, 0.05 eV/Å and 0.1 GPa, respectively.

Table S1. Crystallite size of BiOBr and 5% Co-BiOBr samples by using Debye-Scherrer.

lattice plane of BiOBr	FWHM	crystallites size	average crystallite size	lattice plane of 5% Co-BiOBr	FWHM	crystallites size	average crystallite size
(102)	0.18502	43.50754		(102)	0.28215	28.53527	
(110)	0.23713	34.44091		(110)	0.37709	21.66211	
(200)	0.18057	45.28657	39.64738	(200)	0.24384	33.54391	27.90368
(212)	0.20388	41.89814		(212)	0.27292	31.30949	
(101)	0.27026	33.10375		(101)	0.36579	24.46761	

Table S2. Comparison of the photocatalytic performance of related catalysts in the degradation of CBZ.

Catalyst	Catalyst weight	Details of Catalytic Experiments	Removal efficiency	Ref.
5% Co-BiOBr	20 mg	Xe lamp (300 W, $\lambda > 350$ nm), 10 mg/L CBZ	92.1% (60min)	This work
Cu ₂ O/ZnO@ PET	20 mg	UV, T=52°C, 1.0 mg/L CBZ	98.1% (160min)	[1]
Bi ₂ S ₃ /BiFeO ₃	50 mg	Xe lamp (150 W, $\lambda > 400$ nm). 10 mg/L CBZ	95% (120min)	[2]
Fe/TiO ₂	200 mg	Sunlight, T=25°C, 8 mg/L CBZ	98.5% (60min)	[3]
Gd ₂ (WO ₄) ₃	60 mg	A Philips projection lamp (250 W, 532 nm), 10 mg/L CBZ	98% (140min)	[4]
ZnO-GQD	20 mg	natural sunlight irradiation 1.91 mg/L CBZ	94% (70min)	[5]
SrTiO ₃ /Mo ₂ AlB ₂	20 mg	Halogen lamp(500W) 15 mg/L CBZ	87.5% (80min)	[6]

Table S3. Fluorescence lifetime parameters of the samples.

Samples	A_1	τ_1 (ns)	A_2	τ_2 (ns)	Ave. τ (ns)
BiOBr	0.65329	0.85818	0.48171	0.85819	0.858184244
5% Co-BiOBr	1.03974	0.7886	0.05243	4.97058	1.797215

$$I(t) = I(0) + A_1 \exp(-t/\tau_1) + A_2 \exp(-t/\tau_2) \quad (\text{Eq.S1})$$

$$\tau_{ave} = (A_1 \tau_1^2 + A_2 \tau_2^2) / (A_1 \tau_1 + A_2 \tau_2) \quad (\text{Eq.S2})$$

where t represents time, A_1 and A_2 are exponential prefactors, τ_1 represents the carrier lifetime of the radiative energy-transfer process and τ_2 represents the carrier lifetime of the non-radiative energy-transfer process.

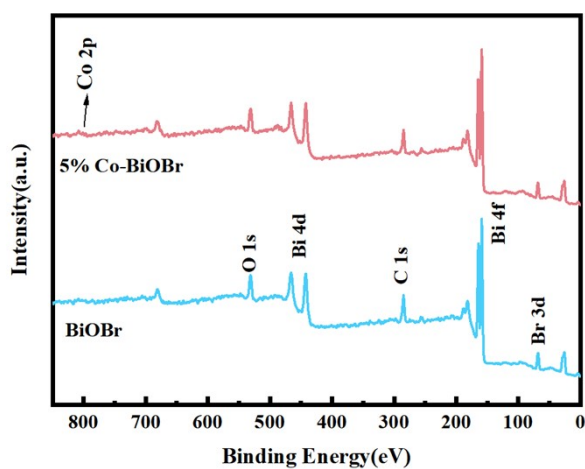


Figure S1. XPS survey spectra of BiOBr and 5% Co-BiOBr.

References

- [1] Altynbaeva, L. S.; Barsbay, M.; Aimanova, N. A.; Jakupova, Z. Y.; Nurpeisova, D. T.; Zdorovets, M. V.; Mashentseva, A. A. A novel Cu₂O/ZnO@PET composite membrane for the photocatalytic degradation of carbendazim[J]. *Nanomaterials*, 2022, 12(10): 1724.
- [2] Bhoi, Y. P.; Nayak, A. K.; Gouda, S. K.; Mishra, B.G. Photocatalytic mineralization of carbendazim pesticide by a visible light active novel type-II Bi₂S₃/BiFeO₃ heterojunction photocatalyst[J]. *Catal. Commun.* 2018, 114: 114-119.
- [3] Kaur T, Sraw A, Wanchoo R K, et al. Solar assisted degradation of carbendazim in water using clay beads immobilized with TiO₂ & Fe doped TiO₂[J]. *Solar Energy*, 2018, 162: 45-56.
- [4] Periyasamy, S.; Kumar, J. V.; Chen, S. M.; Annamala, Y.; Karthik, R.; Rajagounder, N. E. Structural insights on 2D gadolinium tungstate nanoflake: a promising electrocatalyst for sensor and photocatalyst for the degradation of postharvest fungicide (carbendazim)[J]. *ACS. appl. Mater. Interf.* 2019, 11(40): 37172-37183.
- [5] Kumar, S.; Dhiman, A.; Sudhagar, P.; Krishnan, V. ZnO-graphene quantum dots heterojunctions for natural sunlight-driven photocatalytic environmental remediation[J]. *Appl. Surf. Sci.* 2018, 447: 802-815.
- [6] Narendran M G, Peters S, John Bosco A, et al. Pioneering Exploration of Mo₂AlB₂-Transition-Meta-Aluminum-Boron-Phase-Supported Hydrophobic SrTiO₃/Mo₂AlB₂ Nanocomposite for Improved Photocatalytic Carbendazim Degradation and CO₂ Reduction to Ethanol through the Schottky Junction[J]. *Solar RRL*, 2024, 8(8): 2301043.